MECHANISM FOR GEL PROPAGATION THROUGH FRACTURES

R. S. SERIGHT,
New Mexico Petroleum Recovery Research Center-USA

21st ANNUAL INTERNATIONAL ENERGY AGENCY WORKSHOP AND SYMPOSIUM
Edinburgh, Scotland, U.K., September 20-22, 2000

Abstract

This paper considers several mechanistic features of gel extrusion through fractures. During gel extrusion, water leaks off from the gel, and the gel concentrates to become immobile in the vicinity where dehydration occurred. The driving force for gel dehydration (and water leakoff) is the pressure difference between the fracture and the adjacent porous rock. Fresh gel (i.e., mobile gel, with the original composition) must wormhole through the concentrated gel in order to advance the gel front. With time at a given position along the fracture, the average gel concentration increases and the fracture area contacted by wormholes (i.e., mobile gel) decreases. Even so, water leakoff from the concentrated, immobile gel is generally small compared with leakoff from the mobile gel.

A minimum pressure gradient is required to extrude a given gel through a fracture. Once this minimum pressure gradient is exceeded, the pressure gradient during gel extrusion is insensitive to the flow rate. The pressure gradient required for gel extrusion varies inversely with the square of fracture width. In contrast, a force balance during gel extrusion predicts that the pressure gradient should vary linearly with fracture width. Although we have not definitively identified the origin of this behavior, we have demonstrated that it is directly linked to the extremely strong apparent shear-thinning behavior during extrusion. This behavior suggests that a very thin lubricating layer of water at the gel-fracture interface enhances gel extrusion. Apparently, the thickness of the lubricating layer increases with increased superficial velocity.

With an understanding of the mechanism for gel extrusion and dehydration in fractures, we ultimately hope to predict conditions, compositions, and volumes that provide the optimum gel placement in fractured reservoirs. Our work suggests that gels should be injected at the highest practical rate in order to maximize penetration into a fracture system.

Introduction

Gel treatments currently provide the most effective means to reduce channeling through fractures.[1-5] Except in narrow fractures, extruded gels have a placement advantage over conventional gelant treatments. To explain, during conventional gel treatments, a fluid gelant solution typically flows into a reservoir through porous rock and fractures. After placement, chemical reactions (i.e., gelation) cause an immobile gel to form. During gelant injection, fluid velocities in the fracture are usually large enough that viscous forces dominate over gravity forces.[6] Consequently, for small-volume treatments, the gelant front is not greatly distorted by gravity during gelant injection. However, after gelant injection stops, a small density difference (e.g., 1%) between the gelant and the displaced reservoir fluids allows gravity to rapidly drain gelant from at least part of the fracture.[6] Generally, gelation times cannot be controlled well enough to prevent gravity segregation between gelant injection and gelation.

Alternative to conventional gelant treatments, formed gels can be extruded into fractures. Since these gels are 10^3 to 10^6 times mores viscous than gelants, gravity segregation is much less important than for gelants. In fact, for the most successful treatments in fractured reservoirs, formed gels were extruded through fractures during most of the placement process.[2-5] A need exists to determine how much gel should be injected in a given application and where that gel distributes in a fractured reservoir. These parameters depend critically on the properties of gels in fractures. Therefore, we have a research program to determine these properties and to understand how gels extrude through fractures.

Previous Experimental Work

Gels do not flow through porous rock after gelation.[6] This behavior is advantageous since the gel is confined to the fractures—it does not enter or damage the porous rock. Thus, after gel placement, water, oil, or gas can flow unimpeded through the rock, but flow through the fracture is reduced substantially.

However, extrusion of gels through fractures introduces new issues that are not of concern during placement of fluid gelant solutions. First, the pressure gradients required to extrude gels through fractures are greater than those for flow of gelants. For a Cr(III)-acetate-HPAM gel, the pressure gradient required for extrusion varied inversely with the square of fracture width (Figure 1). In previous work,[6-13] we demonstrated that a minimum pressure gradient was required to extrude a given gel through a fracture. Once this minimum pressure gradient was exceeded, the pressure gradient during gel extrusion was insensitive to the flow rate. [6,8]

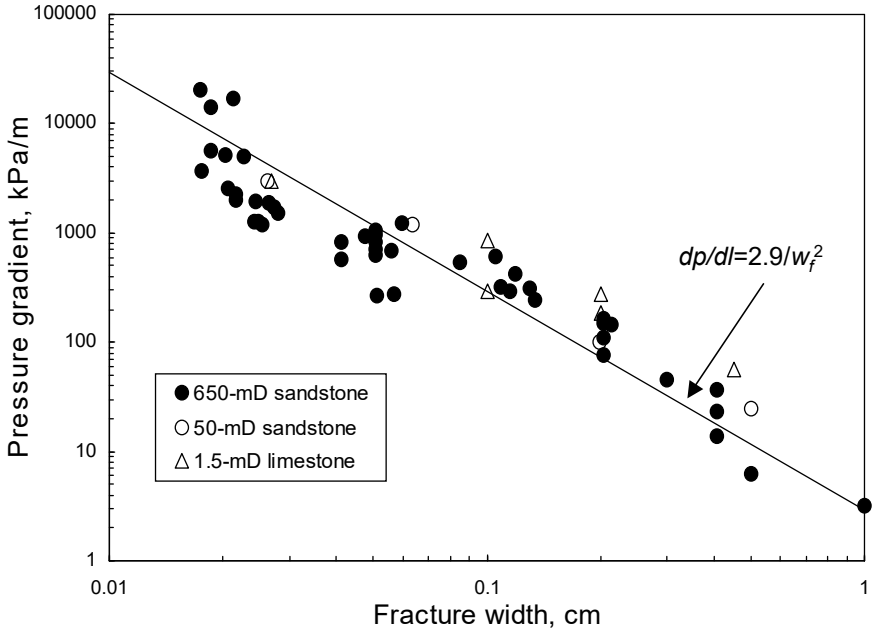

Figure 1—Pressure gradients required for gel extrusion through open fractures.

A second concern is that gels can concentrate (dehydrate) during extrusion through fractures.[9-12] Depending on fracture width (see Figure 2), this dehydration effect can significantly retard gel propagation (e.g., by factors up to 50). Figures 1 and 2 apply to a one-day-old Cr(III)-acetate-HPAM gel at 41°C. This same gel was used for most of the

experiments described in this paper. Specifically, our experiments used an aqueous gel that contained 0.5% Ciba Alcoflood 935 HPAM (molecular weight ≈$5x10^6$ daltons; degree of hydrolysis 5% to 10%), 0.0417% Cr(III) acetate, 1% NaCl, and 0.1% $CaCl_2$ at pH=6. All experiments were performed at 41°C (105°F). The gelant formulations were aged at 41°C for 24 hours (5 times the gelation time) before injection into a fractured core. We designate this gel as our standard Cr(III)-acetate-HPAM gel.

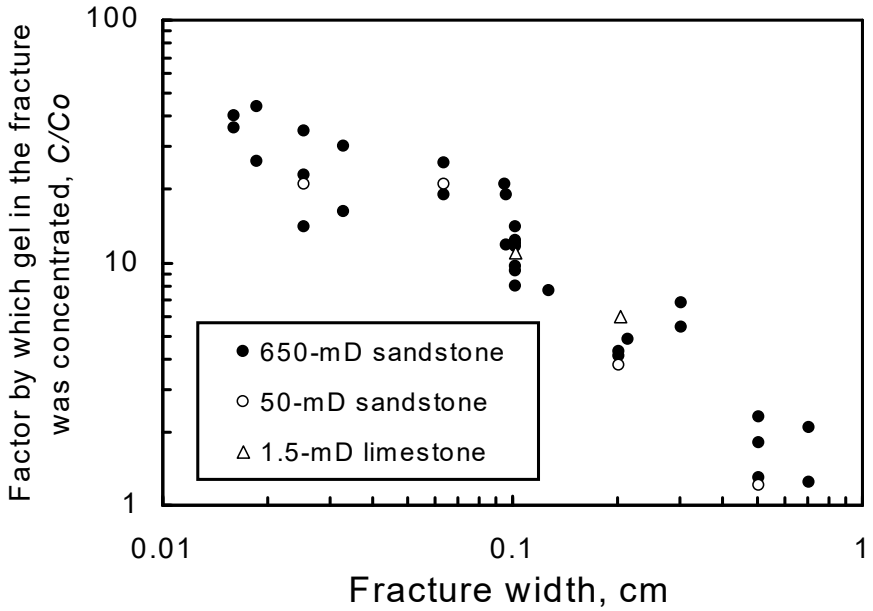

Figure 2—Degree of gel dehydration versus fracture width (from Reference 9).

In earlier work,[9] we showed that when large volumes of gel were extruded through a fracture, progressive plugging (i.e., continuously increasing pressure gradients) was not observed. Effluent from the fracture had the same appearance and a similar composition as those for the injected gel, even though a concentrated, immobile gel formed in the fracture. The concentrated gel formed when water leaked off from the gel along the length of the fracture. The driving force for gel dehydration (and water leakoff) was the pressure difference between the fracture and the adjacent porous rock. During gel extrusion through a fracture of a given width, the pressure gradients along the fracture and the dehydration factors were the same for fractures in 650-mD sandstone as in 50-mD sandstone and 1.5-mD limestone (Figures 1 and 2).

Effect of Injection Rate

Several experiments were performed to examine the effects of injection rate on gel extrusion and dehydration. In each test (at 41°C), we extruded 80 fracture volumes (3,700 cm^3) of our standard 24-hr-old Cr(III)-acetate-HPAM gel through a 0.1-cm-wide fracture in a 122-cm-long, 650-mD Berea sandstone core. The cross-sectional area of the core was 14.5 cm^2 (3.8x3.8 cm), so the fracture height was 3.8 cm. The total fracture volume was 46.5 cm^3, and the total pore volume of the system was about 400 cm^3. The core had five sections of equal length that were delineated by sets of fracture and matrix pressure taps. A fitting at the core outlet separated the effluent from the fracture and matrix. (Of course, a new core was used for each test.) Four tests were performed using gel injection rates of 200, 500, 2,000, and 16,000

cm^3/hr. Assuming that the total fracture volume was open to gel flow, the average velocities ranged from 126 to 10,090 m/d. For comparison, the velocity in a 30-m-high, 0.1-cm-wide, two-wing fracture is 3,700 m/d using an injection rate of 1 barrel per minute (0.16 m^3/min).

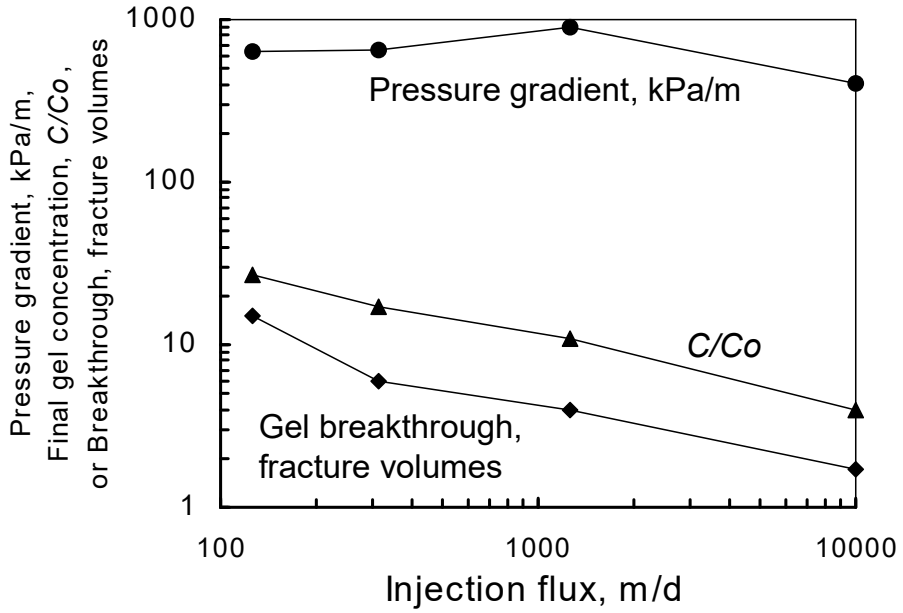

Figure 3—Properties during gel extrusion through 0.1-cm-wide fractures.

Pressure Gradients. Figure 3 summarizes the results from these tests. Consistent with our earlier findings,[6-8] pressure gradients along the fracture were relatively insensitive to injection rate (top curve of Figure 3). The average pressure gradients ranged from 400 to 900 kPa/m for estimated gel velocities ranging from 126 to 10,090 m/d. We suspect the pressure-gradient variations in Figure 3 were caused by differences in the actual fracture width rather than by velocity differences. Mechanical degradation of the gel was fairly small. For gel produced from the fracture at the highest rate, the elastic modulus was about 20% less than that for the original gel. In all cases, the physical appearance of the gel remained unchanged by passage through the fracture.

Gel Front Propagation. The rate of gel front propagation increased significantly with increased injection rate. For 126 m/d, gel arrival at the end of a 122-cm-long fracture occurred after 15 fracture volumes of gel injection (bottom curve of Figure 3). Only 1.7 fracture volumes of gel were required when the velocity was 10,090 m/d. Evidently, the gel had less time to dehydrate as the injection rate increased. With a lower level of gel dehydration (concentration), the gel propagated a greater distance for a given total volume of gel injection. This result has important consequences for field applications. It suggests that gels should be injected at the highest practical rate in order to maximize penetration into the fracture system.

Gel Concentration. After 80 fracture volumes of gel injection, the fracture was opened to reveal a rubbery gel that completely filled the fracture. These gels were analyzed for chromium and HPAM as a function of length along the fracture. The middle curve of Figure 3 shows the average factor by which gel in the fracture was concentrated for each experiment.

Expressed relative to the concentration of the injected gel (C/C_o), gel was concentrated by an average factor of 27 at 126 m/d and by 4 at 10,090 m/d. Of course, since fixed volumes of gel were injected, the duration of gel injection varied inversely with injection rate. Since gel in the fracture was under pressure for a shorter time in the faster experiments, the gel had less time to dehydrate. Consequently, the degree of dehydration decreased with increased injection rate. These results further support our conclusion that in field applications, gels should be injected at the highest practical rate to maximize penetration into the fracture system.

Leakoff. Figure 4 plots the average water leakoff rate (u_l, in $m^3/m^2/d$ or m/d) versus time (t, in days) for eight experiments in 0.1-cm-wide fractures with fracture lengths ranging from 15 to 314 cm and fracture heights ranging from 3.8 to 30.5 cm. At any given time, the average water leakoff rate (from the gel in the fracture into the porous rock) was simply the total flow rate from the matrix (at the end of the core) divided by the total fracture area in the core. Details of this determination can be found in References 10 and 12. Equation 1 provided an excellent fit of the data.

$$u_l = 0.015\, t^{-0.55} \quad \text{..... (1)}$$

Equation 1 provides leakoff rates that are averaged over the length of the fracture (more specifically, over the gel-contacted length of the fracture). Equation 2 relates the average leakoff rate to the local leakoff rate, u_i, at a given distance, L, along the fracture.

$$u_l = \int u_i\, dL / L \quad \text{..... (2)}$$

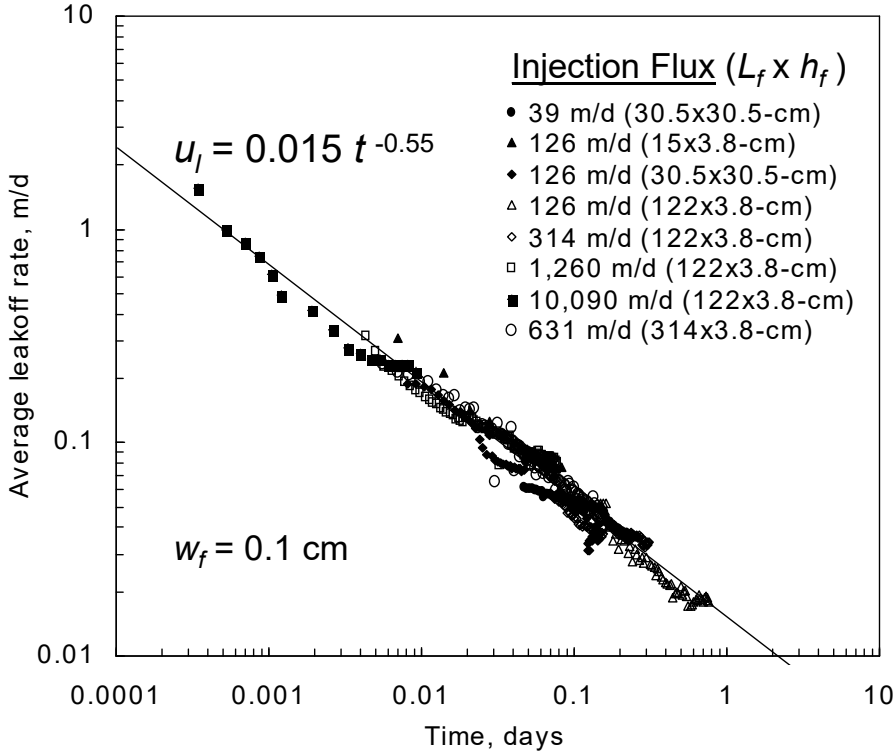

Figure 4—Average leakoff rates during gel injection into 0.1-cm-wide fractures.

Wormholes

Two experiments were performed using fractures that had dimensions of 30.5x30.5x0.1 cm. (Detailed descriptions of these fractured cores can be found in Reference 10.) In one experiment, 30 fracture volumes of our standard 24-hr-old gel were injected at a flux of 39 m/d. In the second experiment, 61 fracture volumes of gel were injected at a flux of 126 m/d. For both experiments, near the end of gel injection, dyed gel of the same composition was injected. For the 39- and 126-m/d experiments, dye breakthrough occurred after 9 cm^3 (0.097 fracture volumes) and 8 cm^3 (0.086 fracture volumes), respectively. At the time of dyed-gel breakthrough, the average gel dehydration factors for newly injected gel were 55% and 17%, respectively (because these were the fractions of total flow produced as water from the end of the matrix). Thus, the estimated volumes of the pathways for the dyed gel were 4 cm^3 [i.e., 9x(1-0.55)] or 0.044 fracture volumes for the 39-m/d experiment and 6.6 cm^3 [i.e., 8x(1-0.17)] or 0.071 fracture volumes for the 126-m/d experiment. These results suggest that the injected gel formed small-volume wormholes through concentrated gel.

Consistent with this suggestion, wormhole pathways were noted (highlighted by the dye) through the concentrated gel in the fracture after opening the fracture at the end of the experiments (Figure 5). The largest of these wormholes were 0.2 to 0.5 cm in height, compared to the total fracture height of 30.5 cm. In the 39-m/d experiment, one wormhole in the center of the pattern appeared dominant, while six other significant wormholes were present in various locations. A limited amount of branching was noted on these wormholes. In contrast, for the 126-m/d experiment, highly branched wormhole patterns were found after dye injection. For both experiments, after removing the gel from the fractures, streaks of dyed rock were noted under the wormholes—revealing the leakoff pathways for water that dehydrated from the gel (Figure 6).

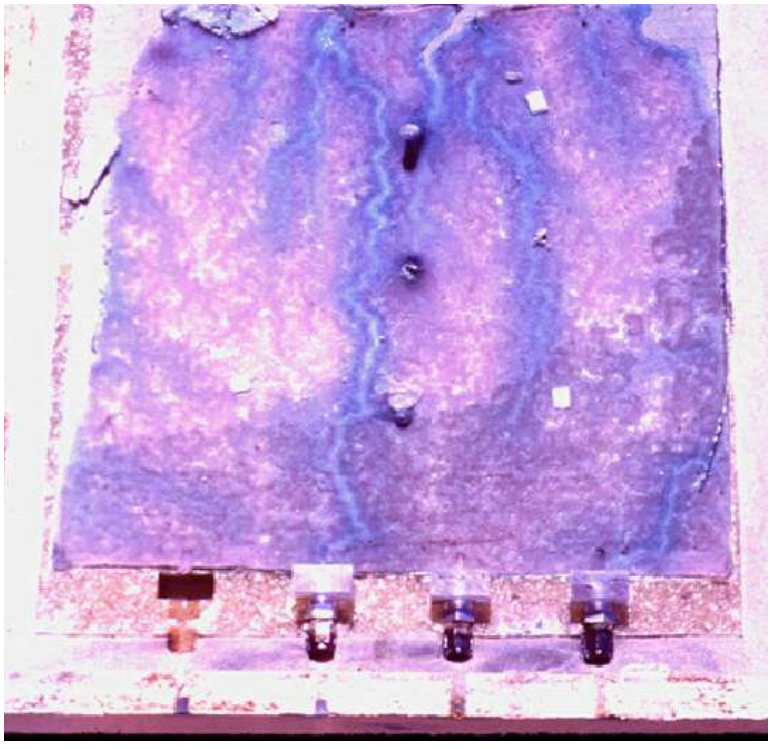

Figure 5—Wormhole pattern after dyed gel injection at 39 m/d. Total gel=30 fracture volumes. Concentrated gel in place. Flow was top to bottom.

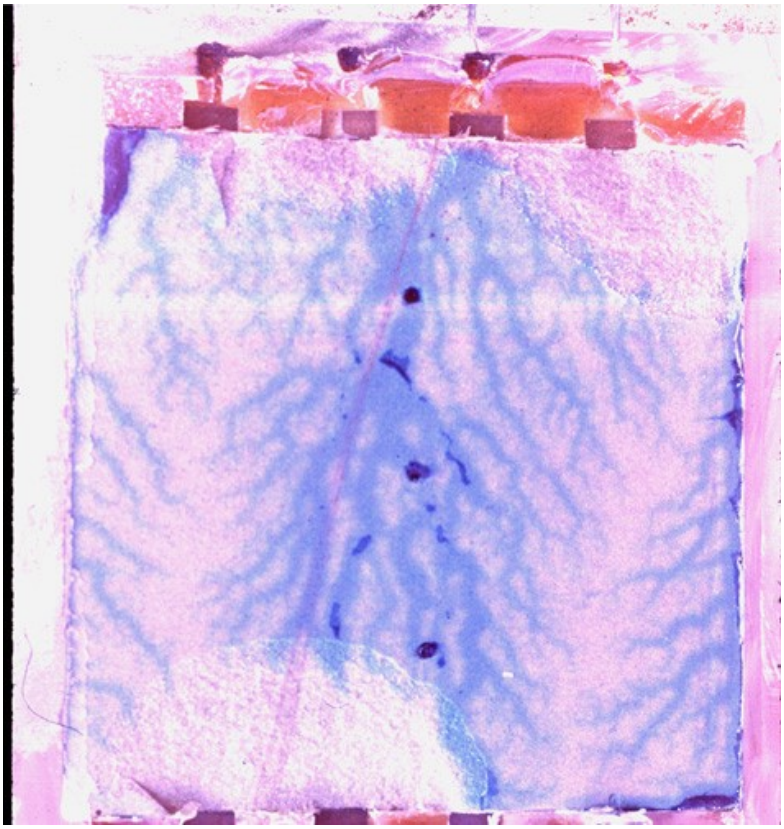

Figure 6—Wormhole pattern after dyed gel injection at 126 m/d. Total gel=61 fracture volumes. Concentrated gel removed to reveal dye leakoff pattern. Flow was top to bottom.

Dyed-gels were also injected near the end of the 314-m/d and 1,260-m/d experiments in the 122x3.8x0.1-cm. fractures. Results indicated that the wormhole volumes were 0.10 and 0.14 fracture volumes, respectively. Since the wormhole volumes were 4% to 14% of the fracture volume, actual velocities for the flowing gel in the wormholes were 7 to 22 times faster than indicated by our flux values (i.e., calculated assuming that the entire fracture cross-section was open to flow).

Physical Basis for Equation 1

What is the physical basis for Equation 1? Because leakoff varies approximately with the reciprocal of the square root of time, one might guess that the relation is analogous to the formation of a filter cake during hydraulic fracturing.[14] However, important differences exist. For normal (incompressible) filter cake formation, a cake forms with permeability, k, and uniform thickness, L. For a given pressure difference, Δp, and solvent viscosity, μ, the solvent flux (leakoff rate), u, through the filter cake is given by the Darcy equation.

$$u = k\Delta p/(\mu L) \quad (3)$$

The filter cake thickness increases with solvent throughput according to Equation 4.

$$L = C_f \int u\, dt \quad (4)$$

Combining Equations 3 and 4, the leakoff rate is easily shown to vary inversely with the square root of time.[14] However, in our problem, where water leakoff occurs during gel extrusion through a fracture, a filter cake of uniform thickness does not form. In particular, we have not observed a gel concentration variation (i.e., a filter cake) in the width direction of the fracture. In contrast, we have noted gel concentration variations along the length and height directions. These latter variations were caused by mobile gel (with a composition of the originally injected gel) that wormholed through immobile, concentrated (dehydrated) gel.[9,12]

Our current picture of the gel propagation and dehydration process is as follows: When the gel front first contacts a new element of fracture area, the gel in this vicinity basically has the same composition as that for the originally injected gel.[9,12] The permeability of this gel to water is relatively high—around 1 mD.[10] Consistent with these observations, the rate of water leakoff (i.e., leakoff flux) from the gel (and fracture) is greatest just upstream of the gel front.[9] As the water leaks off from the gel, the gel concentrates and becomes immobile in the vicinity where the dehydration occurs. The next element of fresh (mobile) gel must find its way around or through (i.e., wormhole through) the concentrated gel in order to advance the gel front. With time at a given position along the fracture, our experiments reveal that the average gel concentration increases and the fracture area contacted by wormholes (i.e., mobile gel) decreases.[9,12]

At any given distance along the length of a fracture, a fraction of the fracture area will be contacted by immobile, concentrated gel, while the remaining area will be contacted by mobile gel (where the wormholes exist). Thus, two separate sources contribute to leakoff—(1) concentrated, immobile gel that was formed from the dehydration process and (2) mobile gel. The leakoff rate (u_l) at any position along a fracture is the sum of leakoff from the mobile gel and the immobile gel. In turn, the average leakoff rate is proportional to the fracture area contacted by mobile (fresh) gel (a_f) and immobile (concentrated) gel (a_c) and the local leakoff rates from the mobile gel (u_f) and the immobile gel (u_c).

$$u_l = a_f u_f + a_c u_c \quad \text{.....(5)}$$

The immobile gel continually concentrates during the extrusion process.[9] We believe that this contribution is minor for the vast majority of the extrusion process because gel permeability to water varies inversely with the third power of gel concentration.[10]

$$u_c = u_f (C/C_o)^{-3} \text{.....(6)}$$

As the immobile gel in the fracture becomes more concentrated, its ability to squeeze out additional water rapidly decreases. Furthermore, experimental studies (using leakoff of dyed water), demonstrated that the dominant source of leakoff was from the mobile gel in the wormholes.[10,12] When an element of mobile gel dehydrates, presumably a thin filter cake of concentrated gel forms on the fracture wall. However, because we have never physically observed this thin layer, we assume that it must be quickly torn and swept to the side (by water trying to reach the fracture face) to merge with the concentrated immobile gel.

Given that the second term in Equation 5 is negligible, the rate of leakoff is determined mainly by leakoff from fresh (mobile) gel in the wormholes.

$$u_l \approx a_f u_f \text{.....(7)}$$

Since the gel in the wormholes is continually replenished, the local leakoff rate, u_f, remains relatively constant during the extrusion process. This fact (along with Equations 1 and 7) implies that the fracture area contacted by wormholes must vary with $t^{-0.55}$. Figure 4 indicates that the leakoff rate should be 2.4 m/d at 0.0001 days. Somewhat arbitrarily, we choose a_f to have a value of one at this time. Thus, Equation 8 provides a credible relation for a_f at times greater than 0.0001 days (~9 seconds).

$$a_f = (0.00625)\, t^{-0.55} \quad \text{.....(8)}$$

This equation is plotted on the left side of Figure 7. The right side of Figure 7 plots the fraction of the fracture area that was contacted by concentrated gel (a_c) versus time. These plots indicated that after 0.0004 days (30 seconds) of gel contact, most of the fracture face is covered by concentrated gel rather than fresh gel.

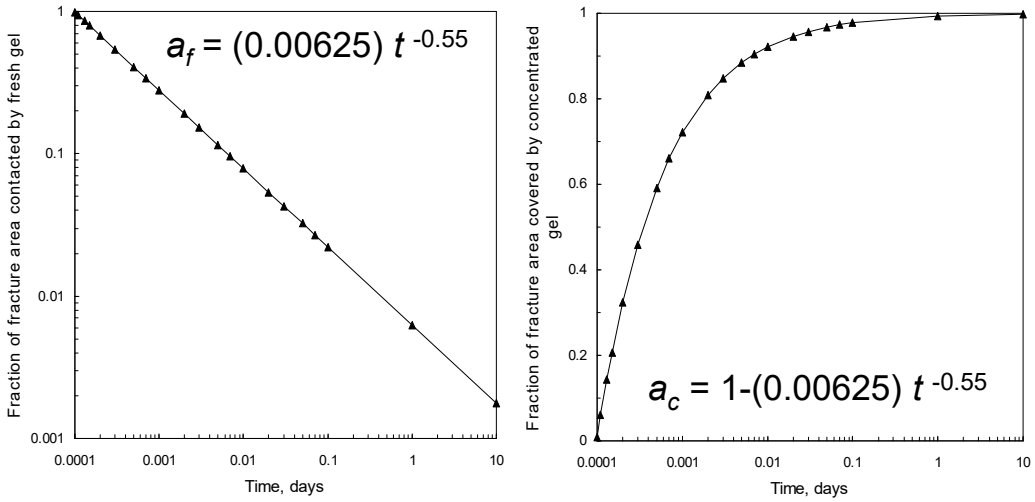

Figure 7—Predictions of fraction of fracture area contacted by fresh versus concentrated gel.

Given that gel becomes immobile after it dehydrates, a mass balance can be used to determine the average concentration as a function of time.

$$C/C_o = 2 \int u_l\, dt / w_f \quad \text{.....(9)}$$

Combining Equations 1 and 9 leads to Equation 10 (when w_f is expressed in centimeters).

$$C/C_o = 6.67\, t^{0.45} / w_f \quad \text{.....(10)}$$

This equation is plotted in Figure 8. In a 0.1-cm-wide fracture, the average gel concentration is predicted to be 3, 10, and 30 after 1.5 minutes, 22 minutes, and 4.2 hours, respectively.

Earlier, we suggested that the leakoff contribution from immobile gel would be negligible. To test this assumption, Equation 6 was combined with Equation 10 to generate Equation 11 and Figure 9. (w_f is expressed in centimeters, u_c has units of m/d, and t is in days.)

$$u_c = 0.0081\, t^{-1.35}\, (w_f)^3 \quad \text{.....(11)}$$

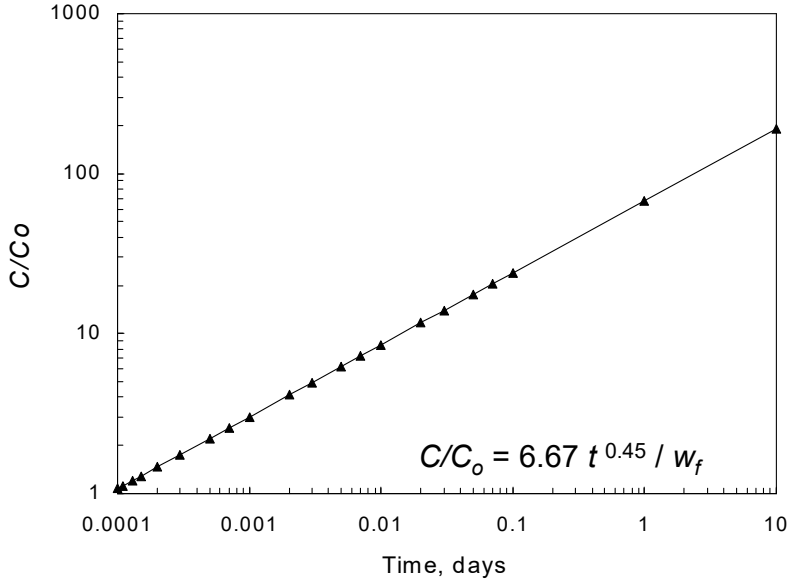

Figure 8—Gel concentration versus time (w_f = 0.1 cm).

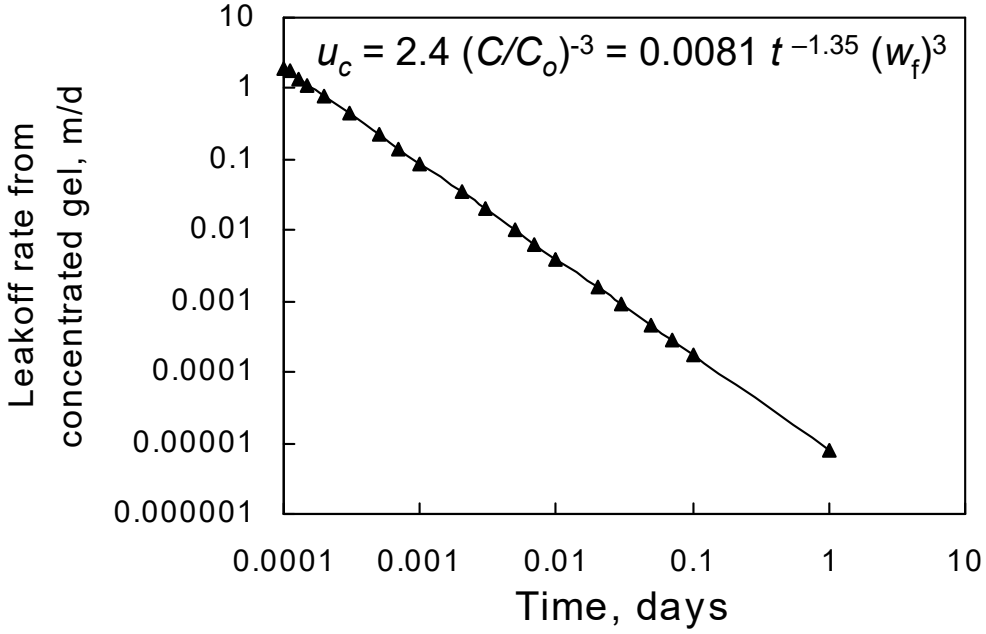

Figure 9—Leakoff rate from concentrated gel (w_f = 0.1 cm).

For w_f = 0.1 cm, Figure 9 demonstrates how rapidly leakoff diminishes from concentrated gel. Consideration of Figures 7 and 9 raises the question, at a given point in a fracture, how does the overall leakoff contribution from fresh gel compare with that from concentrated gel? This point is addressed by plotting the ratio, $a_f u_f / a_c u_c$. This ratio can be determined by combining Equations 8 and 11. Equation 12 was used to generate Figure 10.

$$a_f u_f / a_c u_c = (0.00625)\, t^{-0.55} (2.4) / \{[1 - (0.00625)\, t^{-0.55}][\, 0.0081\, t^{-1.35} (w_f)^3]\} \quad \text{.....(12)}$$

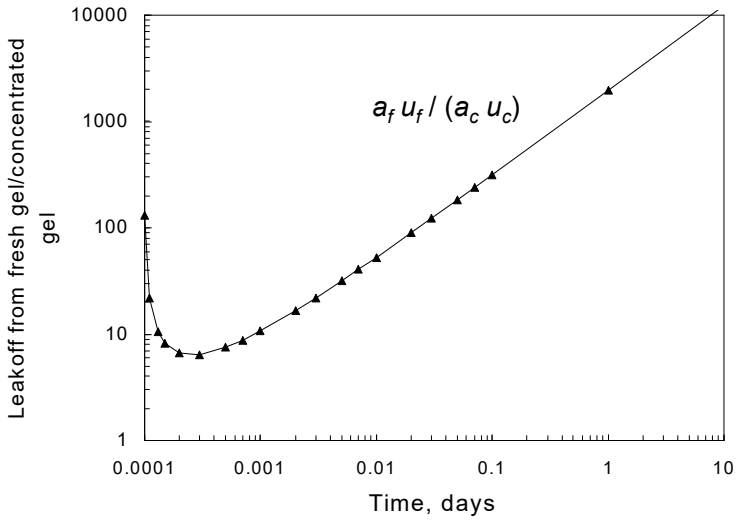

Figure 10—Leakoff from fresh gel relative to concentrated gel (w_f = 0.1 cm).

The above figure shows that at any given point and time along a fracture, the total leakoff from fresh gel is significantly greater than that from the concentrated gel. For a contact time of 0.0003 days (26 seconds), the ratio, $a_f\ u_f\ /\ a_c\ u_c$, reached a minimum value of 6.5. Thereafter, the ratio rose continuously—confirming that leakoff from the concentrated gel became progressively less significant.

$1/(w_f)^2$ Dependence for Pressure Gradients

The pressure gradient required for gel extrusion varies roughly inversely with the square of fracture width (Equation 13 and Figure 1):

$$dp/dl = 2.9 / (w_f)^2 \quad \text{,} \qquad (13)$$

where dp/dl has units of kPa/m and w_f has units of cm. Admittedly, a significant amount of data scatter exists in Figure 1.

Equation 13 fits the data much better than relations based on standard yield-stress analysis. For a material with a yield stress, τ_y, a simple force balance predicts[10] that the pressure gradient required for extrusion should be given by Equation 14.

$$dp/dl = 2\tau_y / w_f \qquad (14)$$

Figure 11 compares the data fit for relations using $1/w_f$ versus using $1/(w_f)^2$. In particular for Equation 14, $2\tau_y$ was assigned a value of 28.7 kPa-cm/m. The $1/(w_f)^2$ relation provided a much better fit than the $1/w_f$ relation.

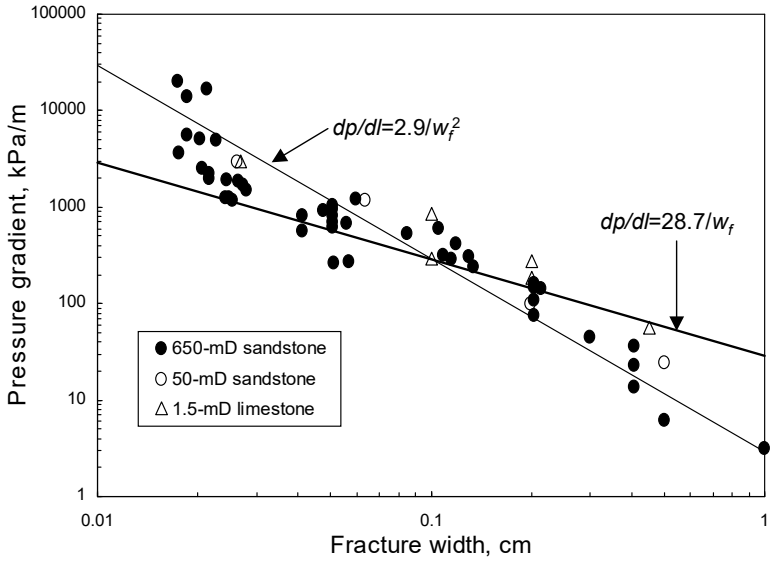

Figure 11—Comparison of $1/(w_f)^2$ versus $1/w_f$ relations.

Relation Between Shear-Thinning and $1/(w_f)^2$ Dependence for Pressure Gradients

Although a relation is not yet evident between the pressure gradient for gel extrusion through a fracture and yield stress in a viscometer, a relation does exist between pressure gradient for gel extrusion and shear-thinning behavior observed in fractures and tubes. In earlier work,[7] we found that gels show an extremely strong apparent shear-thinning behavior when extruding through fractures and tubes. In particular, Figure 12 shows that the gel resistance factor, F_r, (apparent viscosity relative to water) in the fracture decreases substantially with increased superficial velocity, u, (i.e., fluid flux in the fracture). The slope of the data plotted in Figure 12 is in the range from –0.83 to –0.95. In other words, the data in Figure 12 can be approximated using Equation 15.

$$F_r = c_a\, u^n, \quad \ldots\ldots (15)$$

where c_a is a constant, and n is the flux exponent (i.e., –0.83 to –0.95).

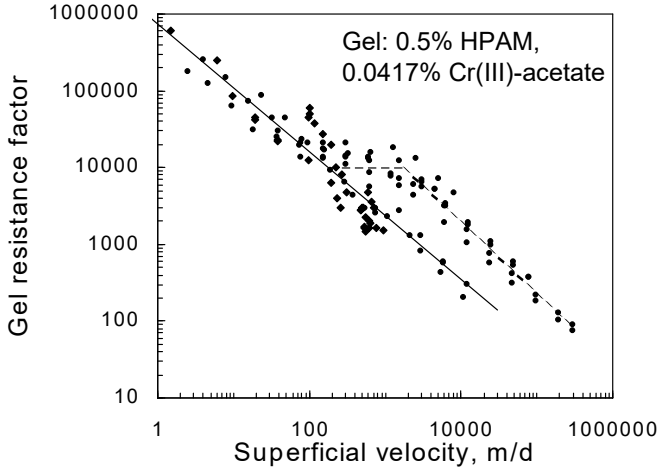

Figure 12—Correlating behavior in short tubes (1 to 5 m) and short fractures (0.15 to 1.2 m). (After Reference 7.)

The steep slopes of the curves in Figure 12 indicate that the pressure gradient is fairly insensitive to fluid velocity over much of the flux range. This fact was demonstrated explicitly in Figure 4 of Reference 7. It can be understood simply by combining Equation 15 with the Darcy equation.

$$dp/dl = u\mu/k_f = u\mu_w F_r / k_f = u^{(n+1)} c_a\mu_w/k_f \quad (16)$$

Since the flux exponent, n, is nearly –1, Equation 16 reduces to Equation 17.

$$dp/dl \approx c_a\mu_w/k_f \quad (17)$$

Since fracture permeability is proportional to the square of fracture width[8], Equation 17 can be transformed to Equation 18.

$$dp/dl \approx c_a c_b \mu_w/(w_f)^2 \quad (18)$$

where c_b is a constant. When the appropriate constants and conversion factors are used, Equation 18 is revealed to be equivalent to Equation 13.

Equations 16, 17, and 18 indicate that the pressure gradient is basically independent of flow rate. For gel to flow in a given fracture, Equations 16, 17, and 18 predict that about the same pressure gradient is required for a near-zero flow rate as that when high flow rates are used. This suggestion is consistent with our observations that gel will not enter a fracture if the pressure gradient is not sufficiently high.[8]

Equation 13 was based on experiments where injection rates were held constant, but fracture widths varied widely (Figure 1). In contrast, Equations 17 and 18 were derived from experiments where fluxes (superficial velocities) varied over a wide range (Figure 12). The success of these equations in describing the experimental results follows directly from our observation that for a given fracture width and conductivity, a minimum pressure gradient is required for gel extrusion.

Our results suggest that a Bingham model might be appropriate when describing extrusion of gels through fractures. In the Bingham rheological model,[15] the fluid will not move until a minimum shear stress or "yield" stress, τ_y, is exceeded. Above this minimum shear stress, the model assumes that flow is basically Newtonian. In the Bingham model, the fluid velocity profile is flat (the velocity gradient is zero) between the center of the fracture and some distance, x_o, from the fracture center. In other words, the gel flows like a solid plug in this region. Between x_o and the fracture wall, the Bingham model assumes Newtonian flow. In effect, the Bingham model assumes that a Newtonian fluid flowing near the fracture wall lubricates the flow of the plug through the fracture. In our experiments, since the gel dehydrates as it extrudes through fractures, we suspect that the water leaving the gel during the dehydration process may be the key component of the lubricating layer.

In Appendix F of Reference 16, an analysis was performed using the Bingham model to determine x_o as a function of gel resistance factor. Equation 19 provides this relation.

$$F_r = 1/[1 - 3(x_o/w_f) + 4(x_o/w_f)^3] \quad (19)$$

This relation can be coupled with Equation 15 to provide an estimate of the thickness of the lubricating layer relative to the fracture width. (Appendix F of Reference 16 shows details of this determination.) Figure 13 shows the results.

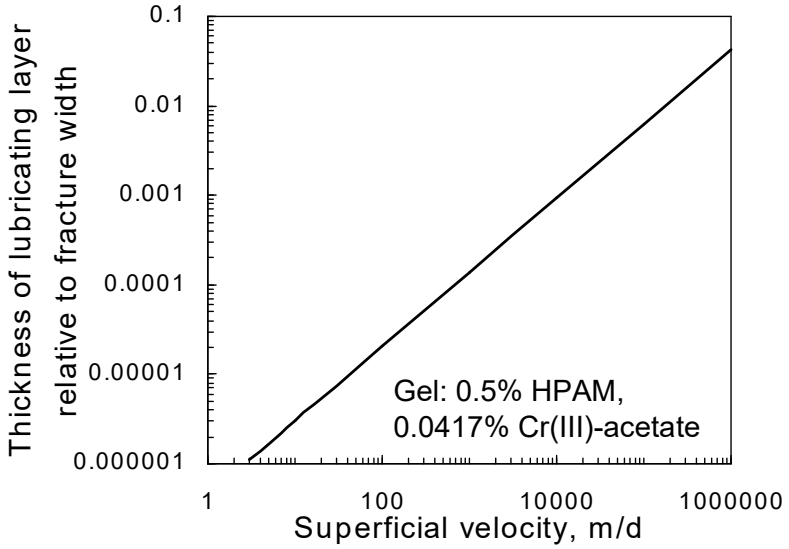

Figure 13—Use of the Bingham model to predict the thickness of the lubricating layer based on Figure 12, Equations 15, and 19.

Figure 13 suggests, first, that the relative thickness of the lubricating layer is very small for the range of velocities shown. Second, the thickness of the lubricating layer increases with increased superficial velocity. If a means could be devised to physically measure the thickness of the lubricating layer (perhaps using interferometry or electric conductivity), one could test whether the thickness of the lubricating layer actually does increase with increased velocity.

Summary

In this paper, we examined several mechanistic features of gel extrusion through fractures. Our current picture of gel propagation is as follows: When the gel front first contacts a new element of fracture area, the gel in this vicinity basically has the same composition as that for the originally injected gel. The permeability of this gel to water is relatively high—around 1 mD. As water leaks off from the gel, the gel concentrates and becomes immobile in the vicinity where dehydration occurred. The driving force for gel dehydration (and water leakoff) is the pressure difference between the fracture and the adjacent porous rock. The next element of fresh (mobile) gel must find its way around or through (i.e., wormhole through) the concentrated gel in order to advance the gel front. With time at a given position along the fracture, the average gel concentration increases and the fracture area contacted by wormholes (i.e., mobile gel) decreases. Even so, water leakoff from the concentrated, immobile gel is generally small compared with leakoff from the mobile gel.

A minimum pressure gradient is required to extrude a given gel through a fracture. Once this minimum pressure gradient is exceeded, the pressure gradient during gel extrusion is insensitive to the flow rate. Stated another way, gels show an extremely strong apparent shear-thinning behavior when extruding through fractures and tubes. The pressure gradient required

for gel extrusion varies roughly inversely with the square of fracture width. In contrast, a force balance during gel extrusion predicts that the pressure gradient should vary linearly with fracture width. Although we have not definitively identified the origin of this behavior, we have demonstrated that it is directly linked to the extremely strong apparent shear-thinning behavior during extrusion. This behavior suggests that a very thin lubricating layer of water at the gel-fracture interface enhances gel extrusion. Apparently, the thickness of the lubricating layer increases with increased superficial velocity.

With an understanding of the mechanism for gel extrusion and dehydration in fractures, we ultimately hope to predict conditions, compositions, and volumes that provide the optimum gel placement in fractured reservoirs. Our work suggests that gels should be injected at the highest practical rate in order to maximize penetration into a fracture system.

Nomenclature

a_c = fraction of fracture area contacted by concentrated gel
a_f = fraction of fracture area contacted by fresh gel
C = produced tracer concentration, g/m^3
C_f = constant in Equation 4
C_o = injected tracer concentration, g/m^3
c_a = constant in Equation 15
c_b = constant in Equation 18
F_r = resistance factor (brine mobility before gel placement divided by gel mobility)
h_f = fracture height, m
k = permeability, darcys [μm^2]
k_f = fracture permeability, darcys [μm^2]
L = distance along a fracture, ft [m]
L_f = fracture length, ft [m]
l = length, m
n = exponent in Equation 15
p = pressure, kPa
dp/dl = pressure gradient, kPa/m
Δp = pressure drop, Pa
u = flux or superficial velocity, m/d
u_c = water leakoff rate from concentrated gel, m/d
u_f = water leakoff rate from fresh gel, m/d
u_i = local water leakoff rate, m/d
u_l = water leakoff rate, m/d
t = time, days
w_f = fracture width, ft [m]
x_o = thickness of a lubricating layer, m
μ = viscosity, cp [Pa-s]
μ_w = viscosity of water, cp [Pa-s]
τ_y = yield stress, Pa

Acknowledgments
Financial support for this work is gratefully acknowledged from the National Petroleum Technology Office of the United States Department of Energy, BP-Amoco, Chevron, China National Petroleum Corp., Chinese Petroleum Corp., Halliburton, Marathon, Norsk Hydro

(Saga), Shell, and Texaco. I thank Richard Schrader and Kate Wavrik for performing the experiments.

References

1. Seright, R.S. and Liang, J.: "A Survey of Field Applications of Gel Treatments for Water Shutoff," paper SPE 26991 presented at the 1994 SPE III Latin American & Caribbean Petroleum Engineering Conference, Buenos Aires, Argentina, April 27-29.
2. Sydansk, R.D. and Moore, P.E.: "Gel Conformance Treatments Increase Oil Production in Wyoming," *Oil & Gas J.* (Jan. 20, 1992) 40-45.
3. Borling, D.C.: "Injection Conformance Control Case Histories Using Gels at the Wertz Field CO_2 Tertiary Flood in Wyoming, USA," paper SPE 27825 presented at the 1994 SPE/DOE Symposium on Improved Oil Recovery, Tulsa, April 17-20.
4. Hild, G.P. and Wackowski, R.K.: "Reservoir Polymer Gel Treatments To Improve Miscible CO_2 Flood," *SPEREE* (April. 1999) 196-204.
5. Lane, R.H. and Sanders, G.S.: "Water Shutoff Through Fullbore Placement of Polymer Gel in Faulted and in Hydraulically Fractured Producers of the Prudhoe Bay Field," paper SPE 29475 presented at the 1995 SPE Production Operations Symposium, Oklahoma City, April 2-4.
6. Seright, R.S.: "Gel Placement in Fractured Systems," *SPEPF* (Nov. 1995), 241-248.
7. Seright, R.S.: "Use of Preformed Gels for Conformance Control in Fractured Systems," *SPEPF* (Feb. 1997) 59-65.
8. Seright, R.S: "Polymer Gel Dehydration During Extrusion Through Fractures," *SPEPF* (May 1999) 110-116.
9. Seright, R.S: "Mechanism for Gel Propagation Through Fractures," paper SPE 55628 presented at the 1999 SPE Rocky Mountain Regional Meeting, Gillette, May 15-19.
10. Seright, R.S.: "Using Chemicals to Optimize Conformance Control in Fractured Reservoirs," Annual Technical Progress Report (U.S. DOE Report DOE/BC/15110-2), U.S. DOE Contract DE-AC26-98BC15110, (Sept. 1999) 3-52.
11. Seright, R.S.: "Improved Methods for Water Shutoff," Final Technical Progress Report (U.S. DOE Report DOE/PC/91008-14), U.S. DOE Contract DE-AC22-94PC91008, BDM-Oklahoma Subcontract G4S60330 (Oct. 1998) 21-54.
12. Seright, R.S.: "Gel Propagation Through Fractures," paper SPE/DOE 59316 presented at the 2000 SPE/DOE Symposium on Improved Oil Recovery, Tulsa, April 2-5.
13. Seright, R.S. and Lee, R.L.: "Gel Treatments for Reducing Channeling Through Naturally Fractured Reservoirs," *SPEPF* (Nov. 1999) 269-276.
14. Howard, G.C. and Fast, C.R.: *Hydraulic Fracturing*, SPE Monograph Series, **2,** Society of Petroleum Engineers, Dallas (1970) 33.
15. Bird, R.B., Stewart, W.E., and Lightfoot, E.N.: *Transport Phenomena*, John Wiley & Sons, New York (1960) 11, 42-63.
16. Seright, R.S.: "Improved Methods for Water Shutoff," Annual Technical Progress Report (U.S. DOE Report DOE/PC/91008-4), U.S. DOE Contract DE-AC22-94PC91008, BDM-Oklahoma Subcontract G4S60330 (Nov. 1997) 223-226.